HHS Public Access

Author manuscript

J Biomech. Author manuscript; available in PMC 2016 July 16.

Published in final edited form as:

J Biomech. 2015 July 16; 48(10): 2110–2115. doi:10.1016/j.jbiomech.2015.02.058.

Achilles tendons from decorin- and biglycan-null mouse models have inferior mechanical and structural properties predicted by an image-based empirical damage model

J.A. Gordon[a], **B.R. Freedman**[a], **A. Zuskov**[a], **R.V. Iozzo**[c], **D.E. Birk**[b], and **L.J. Soslowsky**[a,*]

[a] McKay Orthopaedic Research Laboratory, University of Pennsylvania, Philadelphia, PA, USA

[b] Department of Molecular Pharmacology and Physiology, University of South Florida, Tampa, FL, USA

[c] Department of Pathology, Anatomy and Cell Biology, Thomas Jefferson University, Philadelphia, PA, USA

Abstract

Achilles tendons are a common source of pain and injury, and their pathology may originate from aberrant structure function relationships. Small leucine rich proteoglycans (SLRPs) influence mechanical and structural properties in a tendon-specific manner. However, their roles in the Achilles tendon have not been defined. The objective of this study was to evaluate the mechanical and structural differences observed in mouse Achilles tendons lacking class I SLRPs; either decorin or biglycan. In addition, empirical modeling techniques based on mechanical and image-based measures were employed. Achilles tendons from decorin-null ($Dcn^{-/-}$) and biglycan-null ($Bgn^{-/-}$) C57BL/6 female mice (N=102) were used. Each tendon underwent a dynamic mechanical testing protocol including simultaneous polarized light image capture to evaluate both structural and mechanical properties of each Achilles tendon. An empirical damage model was adapted for application to genetic variation and for use with image based structural properties to predict tendon dynamic mechanical properties. We found that Achilles tendons lacking decorin and biglycan had inferior mechanical and structural properties that were age dependent; and that simple empirical models, based on previously described damage models, were predictive of Achilles tendon dynamic modulus in both decorin- and biglycan-null mice.

Keywords

Proteoglycan; Polarized light; SLRP; Tendon/ligament mechanics; Collagen; Extracellular; Matrix

* Correspondence to: McKay Orthopaedic Research Laboratory, University of Pennsylvania, 424 Stemmler Hall, 3450 Hamilton Walk, Philadelphia, PA 19104-6081, USA. Tel.: +1 215 898 8653; fax: +1 215 573 2133. soslowsk@upenn.edu (L.J. Soslowsky)..

Appendix A. Supporting information

Supplementary data associated with this article can be found in the online version at http://dx.doi.org/10.1016/j.jbiomech.2015.02.058.

1. Introduction

Acute Achilles tendon injuries are estimated at 2.5 million per year in North America (Suchak et al., 2005), with chronic pathology affecting 4% of the general population and exceeding a 60% lifetime risk for certain athletic groups (Jarvinen et al., 2005). The primary diagnosis of acute and chronic Achilles tendon pathology remains clinical, without the benefit of quantitative metrics that would inform physicians about the risk of injury and guide a return to activity (Chiodo et al., 2010). A better understanding of structure-function relationships in the Achilles tendon will lead to a more complete understanding of Achilles biomechanics and may provide opportunities to improve clinical care.

The class I small leucine-rich proteoglycans (SLRPs), decorin and biglycan, are expressed in tendons (Corsi et al., 2002; Young et al., 2002; Ameye et al., 2002; Buckley et al., 2013a, 2013b, 2013c; Danielson et al., 1997; Iozzo, 1998). Both are secreted into the extracellular space where they interact directly with collagen fibrils (Pogány and Vogel, 1992; Iozzo, 1998; Pogány et al., 1994), and contribute to developmental processes (Iozzo et al., 1999; Dellett et al., 2012), particularly fibrillogenesis (Zhang et al., 2006; Vogel et al., 1984). In decorin- and biglycan-null mouse models their absence has been shown to result in altered tendon structure and mechanics (Young et al., 2002; Danielson et al., 1997; Robinson et al., 2005; Dunkman et al., 2013a, 2013b; Buckley et al., 2013a, 2013b, 2013c; Dourte et al., 2013). The role(s) of class I SLRPs in the Achilles tendon have not been defined. This represents a gap in knowledge of tendon development, as well as in the relationships between tendon structure and function.

SLRPs have been shown to cause alterations in collagen fibril structure (Zhang et al., 2006; Vogel et al., 1984; Dunkman et al., 2013a, 2013b). Therefore, utilizing decorin- and biglycan-null tendons provides a model system to evaluate structure-function relationships. In particular, collagen fiber alignment has been correlated with changes in mechanical properties (Lake et al., 2009; Gimbel et al., 2004; Miller et al., 2012a, 2012b). Clinically, shear wave elastography has demonstrated promise in directly measuring mechanics in vivo, while high frequency ultrasound has demonstrated the ability to evaluate dynamically responsive structural elements. Specifically, ultrasound has been established as a means of measuring collagen fascicle alignment (Aubry et al., 2013; Chen et al., 2013; Riggin et al., 2013). However, collagen fiber alignment has not been used to infer dynamic mechanical properties that would be important in the clinical setting. Empirical models have proven successful in extrapolating dynamic mechanical properties in the cases of damage (Sarah Duenwald-Kuehl, 2012), aging and healing (Buckley et al., 2013a, 2013b, 2013c). However, these models have not been extended for use with image-based inputs or applied to cases of genetic variation. Application of empiric models, using structural or mechanical inputs, to predict dynamic mechanical properties would afford an opportunity to infer clinically meaningful data from measurements made with currently available technology.

The purpose of this study was to define the role of SLRPs in Achilles tendon biomechanics and structure. In addition, previously described damage models (Buckley et al., 2013a, 2013b, 2013c; Sarah Duenwald-Kuehl, 2012) were explored in their ability to be extended from aging and injury to modeling of genetic knockout of decorin and biglycan. In this

study, mice lacking either decorin or biglycan, were used as models of altered tendon structure and function (Robinson et al., 2005; Dunkman et al., 2013a, 2013b; Buckley et al., 2013a, 2013b, 2013c; Dourte et al., 2013). The study tested the hypotheses that: (1) knockout of class I SLRPs alters dynamic mechanics and failure loads; (2) collagen fiber alignment is altered in class I SLRP-null Achilles tendons, with less collagen organization in those lacking SLRPs; and (3) a previously described damage model could be extended in its applications to include genetic variation using both mechanical and structural image-based inputs.

2. Methods

2.1. Study design

Wild type female C57BL/6 (WT), decorin-null ($Dcn^{-/-}$) (Danielson et al., 1997), and biglycan-null ($Bgn^{-/-}$) (Xu et al., 1998) mice at maturity (P=150 days), middle (P=300 days), and old age (P=570 days) were used in this study (IACUC approved). WT mice were obtained from Jackson Laboratories and housed at the University of Pennsylvania or obtained already aged from the colony kept at the National Institute on Aging (Bethesda, Maryland). SLRP-null mice were bred at the University of South Florida and shipped to the University of Pennsylvania as described in previous studies (Dunkman et al., 2013a, 2013b; Buckley et al., 2013a, 2013b, 2013c). Distinctions between mature, middle and old age were based on the previously reported decline in mechanical properties in the patellar tendon between 120 and 570 days (Dunkman et al., 2013a, 2013b). All Achilles tendons were randomized, and, to minimize variation, a single dissector (author JAG) was blinded prior to sample preparation. Briefly, the plantaris tendon was removed at its attachment, and non-tendinous soft tissues were dissected away leaving the proximal Achilles tendon free and the distal insertion intact. Cross-sectional area was measured, and tendons were secured using sandpaper placed 5 mm proximal to the insertion in a manner similar to previously described techniques (Buckley et al., 2013a, 2013b, 2013c). Verhoeff's stain was used to create stain lines at 2 and 4 mm for optical strain measurement. The secured tendon was placed in a custom fixture and loaded on an Instron 5848 Universal Testing system (Instron, Norwood, MA). Gauge length was measured optically at preload prior to testing.

Samples underwent a dynamic mechanical testing protocol as described previously (Dunkman et al., 2013a, 2013b), consisting of (1) preloading to 0.05 N, (2) a preconditioning cycle and (3) stress relaxation at 4%, 6% and 8% strain with a (4) sinusoidal frequency sweep through 0.1, 1, 5, and 10 Hz after reaching the tendon's equilibrium stress at each strain. (5) These steps were followed by a final quasi-static ramp to failure. Force and displacement data were acquired at 1.67 kHz using WaveMaker software (Instron, Norwood, MA) and analyzed using a MATLAB program (Mathworks, Natick, MA).

2.2. Imaging protocol

Alignment maps of the tendon were collected as described (Freedman et al., 2014). Briefly, a custom- built polarized light and imaging system quantified collagen fiber alignment during mechanical testing. The system consists of a linear backlight (Dolan-Jenner, Boxborough, MA), rotating polarized sheets offset by 901 (Edmund Optics), and a camera.

Custom software (National Instruments LabVIEW, Austin, TX) synchronized with analog output signals from the Instron triggered alignment map image capture before and after preconditioning, at the beginning and end of each stress relaxation, and during the quasi-static ramp to failure. To quantify collagen alignment from these images, the signal phase and magnitude were determined to compute the circular standard deviation (CSD) and apparent birefringence (B_{app}) (Freedman et al., 2014). For each test, data was normalized to a wave plate alignment map to control for ambient light intensity. All tendons were examined after testing to determine the mode and region of failure.

2.3. Empirical modeling

A strain-based damage model (Sarah Duenwald-Kuehl, 2012; Lemaitre, 1984) was recently validated for aging and in vivo injury of the murine patellar tendon (Buckley et al., 2013a, 2013b, 2013c). Briefly, the premise of these models is that a tendon damaged by overstretch, aging, or injury reacts to an applied strain as if the strain were lower (Buckley et al., 2013a, 2013b, 2013c). Thus, the damage-dependent effective strain follows the relationship, $\varepsilon_{effective} = \varepsilon_{applied} * (1 - D)$, where $0 < D < 1$ and D is a parameter representing the degree of damage. For the undamaged condition, $D=0$. This definition was adapted for application to genetic variation as well as with the use of image-based measures employed in predicting dynamic mechanical properties. A mechanically based measure was initially used to validate the utility of such models in the context of genetic variation. All models utilized data from the middle age time point, to avoid the potential extremes of age. The damage parameter D for mechanical property inputs was defined according to Eq. (1).

$$1 - D = \frac{\sigma_{eq}^{Genetic\Delta}(6\%\text{strain})}{\sigma_{eq}^{WTControl}(6\%\text{strain})} \quad (1)$$

where σ_{eq} is the stress equilibrium following stress relaxation, in this instance specifically the 6% strain case, and D is the damage parameter defined by the given equation.

A similar equation was created to adapt the model for use with calculated B_{app} according to Eq. (2).

$$1 - D = \frac{B_{eq}^{Genetic\Delta}(6\%\text{strain})}{B_{eq}^{WTControl}(6\%\text{strain})} \quad (2)$$

The remaining terms in our model were determined using power regression as previously described (Buckley et al., 2013a, 2013b, 2013c). Similarly, data from the 6% strain, 1 Hz portion of the testing protocol were used to define the coefficients for the power-law model described by Eq. (3).

$$|E^*|_{Genetic\Delta} = A_i \left[(1 - D) \left\langle |E^*|_{WTControl} \right\rangle \right]^{n_i} \quad (3)$$

where $|E^*|$ is dynamic modulus and n_i and A_i are defined through power regression. Only mechanical properties with significant model fits were used in the analysis. It is noted that the parameters A_i and n_i do not correspond to physical tendon properties, rather they

describe how |*E**| scales with its baseline values and the degree of damage (Buckley et al., 2013a, 2013b, 2013c). In the model, |*E**| was predicted for *Dcn*$^{-/-}$ tendons using model parameters derived from *Bgn*$^{-/-}$ tendons.

2.4. Statistical evaluation

One way ANOVAs were used to determine significant differences across genotypes. Significant relationships were evaluated with post-hoc Student's *T*-tests with Bonferroni corrections ($p<0.05/3$ for each genotype). All significant differences were displayed in figures as solid bars ($p<0.0167$), with trends indicated by dashed lines ($p<0.033$). Pearson's coefficients of determination (R^2) were determined for damage model fits and predictions of dynamic mechanical properties. Power analysis was conducted prior to experimentation based on previous studies (Dunkman et al., 2013a, 2013b) and determined that 12 tendons were required for an $\alpha=0.05$ and $\beta=0.8$.

3. Results

A significant increase in the cross-sectional area of the *Dcn*$^{-/-}$ tendons was observed (Fig. 1A). Despite a larger cross-sectional area, the ultimate load at failure was significantly reduced in the *Dcn*$^{-/-}$ tendons, and further reduced in the *Bgn*$^{-/-}$tendons at maturity, middle and old age (Fig. 1B). All tendon ruptures occurred at the insertion, except one that failed in the midsubstance.

Dynamic mechanical properties were altered for both the *Dcn*$^{-/-}$ and the *Bgn*$^{-/-}$Achilles tendons. WT tendons had a significantly higher |*E**| at maturity and middle age, but the WT |*E**| was not different from that of *Dcn*$^{-/-}$and *Bgn*$^{-/-}$in old age (Figs. 2, S1). P570 WT tendons had a negative percent change in |*E**| ($p<0.05$) when compared to P150 tendons, however this effect with aging was absent in *Dcn*$^{-/-}$and *Bgn*$^{-/-}$tendons (p40.05). Changes in tanδ, a measure of phase shift related to viscous properties of a material, demonstrated relationships that mirrored the findings for |*E**| (Figs. 3, S2). *Dcn*$^{-/-}$tendons were found to have significantly greater viscous properties at maturity and middle age, and *Bgn*$^{-/-}$tendons demonstrated greater viscous properties at maturity when compared to WT tendons. There were no significant differences in |*E**| and tanδ between groups in old age.

Significant differences in image-based measures of collagen fiber alignment were observed between WT and both SLRP-null tendons. B_{app} and CSD, both measures of collagen fiber alignment, showed age-dependent genotypic variation in collagen organization at the insertion (Figs. 4, S3). Overall, the Achilles tendons of WT mice showed greater organization of fibers than those of both SLRP-null tendons. Additionally, data demonstrated internal consistency in that collagen fiber organization responded appropriately and consistently throughout dynamic testing, as reported from previous data (Lake et al., 2010; Freedman et al., 2014).

Empirical modeling was effective in predicting changes in |*E**| resulting from genetic variation. When using equilibrium stress as an input to define the damage coefficient *D*, there was moderate correlation between predicted and measured dynamic moduli at strains of 4%, 6% and 8% strain (Table 1). Overall, with data pooled from different levels of strain,

a moderate correlation between measured and predicted dynamic modulus (R^2=0.66) was observed when using stress equilibria as an input (Fig. 5A). This confirms the usefulness of mathematical models in the evaluation of genetic variation. Image-based inputs used in this model resulted in similar findings (Table 2), with slightly weaker, but still moderate, coefficients of determination between predicted and measured |*E**|. In this case, aggregate data resulted in a coefficient of determination of R^2=0.53, providing further support for the use of structural measures as a valid input for modeling mechanical behavior (Fig. 5B).

4. Discussion

This study defines the mechanical and structural alterations observed with a deficiency of SLRPs in the Achilles tendon. Using these mechanical and structural properties, we successfully applied a simple damage model to predict the |*E**| in *Dcn*$^{-/-}$and *Bgn*$^{-/-}$tendons. Together, these data have potential implications for injury, evaluation and treatment of Achilles tendons.

The first hypothesis was confirmed; tendons deficient in decorin and biglycan had significantly altered dynamic mechanics and failure loads. Inferior failure loads were present in all age groups, thus identifying class I SLRPs as potential regulators of rupture risk. This may have implications for tissue engineering and biologically based treatments. In addition, the |*E**| decreased in mature and middle aged *Dcn*$^{-/-}$ and *Bgn*$^{-/-}$ tendons, further highlighting the role of class I SLRPs in viscoelastic properties (Dunkman et al., 2013a, 2013b). In previous work, hydrolysis of GAG chains with chondroitinase ABC did not alter flexor carpi ulnaris tendon viscoelastic mechanical properties, but the absence of biglycan did, in a region-specific manner (Buckley et al., 2013b). This may support a predominantly developmental role for class I SLRPs in their effect on mechanical measures. This remains consistent with our results and similar to results in *Bgn*$^{-/-}$ flexor digitorum longus tendons (Robinson et al., 2005), however, additional work will be required to evaluate the timing and mechanism of effect that class I SLRPs have on Achilles tendon mechanics. Other heterogeneous mechanical alterations have been observed in *Dcn*$^{-/-}$ and *Bgn*$^{-/-}$ tendons, however, despite consistency between tests of a given tendon type, their impact on viscoelastic mechanical properties is tendon specific (Robinson et al., 2005; Dourte et al., 2013; Buckley et al., 2013a, 2013b, 2013c). Although each specific tendon has a unique set of characteristics, including specific loading environnements, intra- versus extra- synovial anatomic position and altered surrounding anatomy, the specific reason for these differences remains unknown. Regional distribution of SLRPs within tendons may play a role. Although regional differences in proteoglycans and GAGs between tendons and within a single tendon have been noted both biochemically and mechanically (Buckley et al., 2013a, 2013b, 2013c; Matuszewski et al., 2012; Merrilees and Flint, 1980; Rigozzi et al., 2009; Thomopoulos et al., 2003; Kilts et al., 2009), significant work is needed to fully characterize the significance of these relationships.

As WT control tendons aged, their viscoelastic properties approached those of *Dcn*$^{-/-}$ and *Bgn*$^{-/-}$ tendons. In old age, there were no statistical differences in any measure of viscoelastic properties. This reaffirms previous findings that SLRPs may participate in the aging process (Dunkman et al., 2013a, 2013b). Interestingly, differences in ultimate failure

load between genotypes were preserved through old age. Future work is warranted to further characterize the mechanical role of SLRPs in fatigue loading, and failure mechanics (Fessel and Snedeker, 2011).

The second hypothesis was confirmed as significant differences in collagen fiber alignment were observed between WT and SLRP-null tendons. Specifically, decreased collagen organization existed as a result of the deficiency of decorin and biglycan, but this was only detected at the middle age time point. The decrease in fiber alignment in the absence of decorin or biglycan is consistent with the known increase in fiber heterogeneity during fibrillogenesis resulting from congenital absence of class I SLRPs (Zhang et al., 2006; Iozzo, 1998). Further characterization of this relationship may allow imaging techniques to more precisely target the mechanically relevant aspects of structural measures.

Genetic abnormalities and aging have been increasingly implicated in Achilles tendon injury as well as other ligamentous and tendinous pathology (Laguette et al., 2011; Raleigh et al., 2009; Magra and Maffulli, 2008; September et al., 2009). Here, we have been able to extend the use of a simple damage model previously described for use in aged and damaged tendons (Lemaitre, 1984; Buckley et al., 2013a, 2013b, 2013c; Sarah Duenwald-Kuehl, 2012). This model was validated in the case of genetic variation and with the use of image-based inputs. These extensions of previous models are potentially applicable to patients with genetic variation and also for use with image-based evaluation tools, such as ultrasound. Previous studies have indicated that changes in viscoelastic properties resulting from aging and injury were both well-described by this model suggesting that similar underlying mechanisms may be at play (Buckley et al., 2013a, 2013b, 2013c). Based on this previously described relationship (Buckley et al., 2013a, 2013b, 2013c), our data would support further commonality between these conditions and genetic variation as explored in this study. Findings support the use of the model non-specifically for genetic alteration, but further validation with other mutations would strengthen these findings. These results support the concept that many factors including age, genetic variance and degree of damage may alter tendon function; with the effect of each predictable by modeling. Such models can be powerful tools for extrapolation of mechanical behavior at levels that may otherwise jeopardize the tendon with measures at, or near, rest.

This study is not without limitations. First, the present study does not differentiate the impact of SLRPS during development from their role at maturity. The contribution of glycosaminogly-cans to viscoelastic mechanical properties in mature tendons has been the topic of a long-standing debate (Lujan et al., 2009; Robinson et al., 2005; Fessel and Snedeker, 2011, 2009; Screen et al., 2005; Buckley et al., 2013a, 2013b, 2013c). Studies have shown little to no change in viscoelastic mechanical properties after GAG digestion (Buckley et al., 2012; Screen et al., 2005; Fessel and Snedeker, 2011). The creation or use of inducible knockouts at various points during development may address this question. Further, our study did not explore the potential overlapping function of decorin and biglycan where their effects have previously been observed to be additive (Corsi et al., 2002). Use of double knockouts of decorin and biglycan, could address this issue.

With regard to the application of our model to predict function, its simplicity helps to identify basic mechanical properties and structural measures as important factors in dynamic mechanical behavior, however there are multiple other unincorporated factors that are known to alter these mechanical properties. Other contributors may include fibril continuity (Provenzano and Vanderby, 2006), fibril sliding (Screen et al., 2005; Gupta et al., 2010), GAG content (Ahmadzadeh et al., 2013), microstructural organization (Dunkman et al., 2013a, 2013b; Morgan et al., 2006), tendon crimp (Legerlotz et al., 2014; Buckley et al., 2013a, 2013b, 2013c) and other factors. Eventual models may aim to incorporate such varied inputs through multivariate analysis able to more accurately predict behavior. Gender has also been implicated in altering the mechanical and biological behavior of tendons (Bryant et al., 2008; Kubo et al., 2003; Fletcher et al., 2013; Hansen and Kjaer, 2014), and its influence on the differential effects of SLRPs will be a focus of future investigations.

This study joins a body of work (Robinson et al., 2005; Buckley et al., 2013a, 2013b, 2013c; Fessel and Snedeker, 2009, 2011; Dunkman et al., 2013a, 2013b) that supports a strong developmental or homeostatic role for SLRPs. Future work is necessary to determine how these proteins alter biological responses in the Achilles and may lead to a more fundamental understanding of tendon structure-function relationships.

In conclusion, this study defined the roles of SLRPs in the Achilles tendon and used mechanical and image-based structural metrics to predict dynamic mechanical properties. These findings have implications for recent investigations of mechanical and image-based analysis used to evaluate in vivo dynamic mechanical function.

Supplementary Material

Refer to Web version on PubMed Central for supplementary material.

Acknowledgements

We would like to acknowledge our funding sources NSF GRFP and NIH/NIAMS (P30 AR050950). We acknowledge Andrew A. Dunkman for assistance with sample preparation. We also acknowledge the National Institute on Aging for the use of their aged mouse colony, which enabled us to complete this work.

References

Ahmadzadeh H, Connizzo BK, Freedman BR, Soslowsky LJ, Shenoy VB. Determining the contribution of glycosaminoglycans to tendon mechanical properties with a modified shear-lag model. J. Biomech. 2013; 46:2497–2503. [PubMed: 23932185]

Ameye L, Aria D, Jepsen K, Oldberg A, Xu T, Young MF. Abnormal collagen fibrils in tendons of biglycan/fibromodulin-deficient mice lead to gait impairment, ectopic ossification, and osteoarthritis. FASEB J. Off. Publ. Fed. Am. Soc. Exp. Biol. 2002; 16:673–680.

Aubry S, Risson J-R, Kastler A, Barbier-Brion B, Siliman G, Runge M, Kastler B. Biomechanical properties of the calcaneal tendon in vivo assessed by transient shear wave elastography. Skeletal Radiol. 2013; 42:1143–1150. [PubMed: 23708047]

Bryant AL, Clark RA, Bartold S, Murphy A, Bennell KL, Hohmann E, Marshall-Gradisnik S, Payne C, Crossley KM. Effects of estrogen on the mechanical behavior of the human Achilles tendon in vivo. J. Appl. Physiol. (Bethesda, MD). 2008; 1985(105):1035–1043.

Buckley MR, Dunkman AA, Reuther KE, Kumar A, Pathmanathan L, Beason DP, Birk DE, Soslowsky LJ. Validation of an empirical damage model for aging and in vivo injury of the murine patellar tendon. J. Biomech. Eng. 2013a; 135:041005. [PubMed: 24231900]

Buckley MR, Huffman GR, Iozzo RV, Birk DE, Soslowsky LJ. The location-specific role of proteoglycans in the flexor carpi ulnaris tendon. Connect. Tissue Res. 2013b; 54:367–373. [PubMed: 23941206]

Buckley MR, Sarver JJ, Freedman BR, Soslowsky LJ. The dynamics of collagen uncrimping and lateral contraction in tendon and the effect of ionic concentration. J. Biomech. 2013c; 46:2242–2249. [PubMed: 23876711]

Chen X-M, Cui L-G, He P, Shen W-W, Qian Y-J, Wang J-R. Shear wave elastographic characterization of normal and torn achilles tendons: a pilot study. J. Ultrasound Med. Off. J. Am. Inst. Ultrasound Med. 2013; 32:449–455.

Chiodo CP, Glazebrook M, Bluman EM, Cohen BE, Femino JE, Giza E, Watters WC, Goldberg MJ, Keith M, Haralson RH, Turkelson CM, Wies JL, Raymond L, Anderson S, Boyer K, Sluka P. Diagnosis and treatment of acute Achilles tendon rupture. J. Am. Acad. Orthop. Surg. 2010; 18:503–510. [PubMed: 20675643]

Corsi A, Xu T, Chen XD, Boyde A, Liang J, Mankani M, Sommer B, Iozzo RV, Eichstetter I, Robey PG, Bianco P, Young MF. Phenotypic effects of biglycan deficiency are linked to collagen fibril abnormalities, are synergized by decorin deficiency, and mimic Ehlers–Danlos-like changes in bone and other connective tissues. J. Bone Miner. Res. Off. J. Am. Soc. Bone Miner. Res. 2002; 17:1180–1189.

Danielson KG, Baribault H, Holmes DF, Graham H, Kadler KE, Iozzo RV. Targeted disruption of decorin leads to abnormal collagen fibril morphology and skin fragility. J. Cell Biol. 1997; 136:729–743. [PubMed: 9024701]

Dellett M, Hu W, Papadaki V, Ohnuma S. Small leucine rich proteoglycan family regulates multiple signalling pathways in neural development and maintenance. Dev. Growth Differ. 2012; 54:327–340. [PubMed: 22524604]

Dourte LM, Pathmanathan L, Mienaltowski MJ, Jawad AF, Birk DE, Soslowsky LJ. Mechanical, compositional, and structural properties of the mouse patellar tendon with changes in biglycan gene expression. J. Orthop. Res. Off. Publ. Orthop. Res. Soc. 2013; 31:1430–1437.

Dunkman AA, Buckley MR, Mienaltowski MJ, Adams SM, Thomas SJ, Kumar A, Beason DP, Iozzo RV, Birk DE, Soslowsky LJ. The injury response of aged tendons in the absence of biglycan and decorin. Matrix Biol. J. Int. Soc. Matrix Biol. 2013a

Dunkman AA, Buckley MR, Mienaltowski MJ, Adams SM, Thomas SJ, Satchell L, Kumar A, Pathmanathan L, Beason DP, Iozzo RV, Birk DE, Soslowsky LJ. Decorin expression is important for age-related changes in tendon structure and mechanical properties. Matrix Biol. 2013b; 32:3–13. [PubMed: 23178232]

Fessel G, Snedeker JG. Evidence against proteoglycan mediated collagen fibril load transmission and dynamic viscoelasticity in tendon. Matrix Biol. 2009; 28:503–510. [PubMed: 19698786]

Fessel G, Snedeker JG. Equivalent stiffness after glycosaminoglycan depletion in tendon—an ultra-structural finite element model and corresponding experiments. J. Theor. Biol. 2011; 268:77–83. [PubMed: 20950629]

Fletcher JR, Pfister TR, Macintosh BR. Energy cost of running and Achilles tendon stiffness in man and woman trained runners. Physiol. Rep. 1e00178. 2013

Freedman BR, Sarver JJ, Buckley MR, Voleti PB, Soslowsky LJ. Biomechanical and structural response of healing Achilles tendon to fatigue loading following acute injury. J. Biomech. 2014; 47:2028–2034. [PubMed: 24280564]

Gimbel JA, Van Kleunen JP, Mehta S, Perry SM, Williams GR, Soslowsky LJ. Supraspinatus tendon organizational and mechanical properties in a chronic rotator cuff tear animal model. J. Biomech. 2004; 37:739–749. [PubMed: 15047003]

Gupta HS, Seto J, Krauss S, Boesecke P, Screen HRC. In situ multi-level analysis of viscoelastic deformation mechanisms in tendon collagen. J. Struct. Biol. 2010; 169:183–191. [PubMed: 19822213]

Hansen M, Kjaer M. Influence of sex and estrogen on musculotendinous protein turnover at rest and after exercise. Exerc. Sport Sci. Rev. 2014; 42:183–192. [PubMed: 25062001]

Iozzo RV. Matrix proteoglycans: from molecular design to cellular function. Annu. Rev. Biochem. 1998; 67:609–652. [PubMed: 9759499]

Iozzo RV, Moscatello DK, McQuillan DJ, Eichstetter I. Decorin is a biological ligand for the epidermal growth factor receptor. J. Biol. Chem. 1999; 274:4489–4492. [PubMed: 9988678]

Jarvinen TA, Kannus P, Maffulli N, Khan KM. Achilles tendon disorders: etiology and epidemiology. Foot Ankle Clin. 2005; 10:255–266. [PubMed: 15922917]

Kilts T, Ameye L, Syed-Picard F, Ono M, Berendsen AD, Oldberg A, Heegaard A-M, Bi Y, Young MF. Potential roles for the small leucine-rich proteoglycans biglycan and fibromodulin in ectopic ossification of tendon induced by exercise and in modulating rotarod performance. Scand. J. Med. Sci. Sports. 2009; 19:536–546. [PubMed: 19422643]

Kubo K, Kanehisa H, Fukunaga T. Gender differences in the viscoelastic properties of tendon structures. Eur. J. Appl. Physiol. 2003; 88:520–526. [PubMed: 12560950]

Laguette M-J, Abrahams Y, Prince S, Collins M. Sequence variants within the 3′-UTR of the COL5A1 gene alters mRNA stability: implications for musculoskeletal soft tissue injuries. Matrix Biol. J. Int. Soc. Matrix Biol. 2011; 30:338–345.

Lake SP, Miller KS, Elliott DM, Soslowsky LJ. Effect of fiber distribution and realignment on the nonlinear and inhomogeneous mechanical properties of human supraspinatus tendon under longitudinal tensile loading. J. Orthop. Res. Off. Publ. Orthop. Res. Soc. 2009; 27:1596–1602.

Lake SP, Miller KS, Elliott DM, Soslowsky LJ. Tensile properties and fiber alignment of human supraspinatus tendon in the transverse direction demonstrate inhomogeneity, nonlinearity, and regional isotropy. J. Biomech. 2010; 43:727–732. [PubMed: 19900677]

Legerlotz K, Dorn J, Richter J, Rausch M, Leupin O. Age-dependent regulation of tendon crimp structure, cell length and gap width with strain. Acta Biomater. 2014

Lemaitre J. How to use damage mechanics. Nucl. Eng. Des. 1984; 80:233–245.

Lujan TJ, Underwood CJ, Jacobs NT, Weiss JA. Contribution of glycosaminoglycans to viscoelastic tensile behavior of human ligament. J. Appl. Physiol. (Bethesda, MD). 2009; 1985(106):423–431.

Magra M, Maffulli N. Genetic aspects of tendinopathy. J. Sci. Med. Sport Sports Med. Aust. 2008; 11:243–247.

Matuszewski PE, Chen Y-L, Szczesny SE, Lake SP, Elliott DM, Soslowsky LJ, Dodge GR. Regional variation in human supraspinatus tendon proteoglycans: decorin, biglycan, and aggrecan. Connect. Tissue Res. 2012; 53:343–348. [PubMed: 22329809]

Merrilees MJ, Flint MH. Ultrastructural study of tension and pressure zones in a rabbit flexor tendon. Am. J. Anat. 1980; 157:87–106. [PubMed: 7190773]

Miller KS, Connizzo BK, Feeney E, Soslowsky LJ. Characterizing local collagen fiber re-alignment and crimp behavior throughout mechanical testing in a mature mouse supraspinatus tendon model. J. Biomech. 2012a; 45:2061–2065. [PubMed: 22776688]

Miller KS, Edelstein L, Connizzo BK, Soslowsky LJ. Effect of preconditioning and stress relaxation on local collagen fiber re-alignment: inhomogeneous properties of rat supraspinatus tendon. J. Biomech. Eng. 2012b; 134:031007. [PubMed: 22482687]

Morgan M, Kostyuk O, Brown RA, Mudera V. In situ monitoring of tendon structural changes by elastic scattering spectroscopy: correlation with changes in collagen fibril diameter and crimp. Tissue Eng. 2006; 12:1821–1831. [PubMed: 16889512]

Pogány G, Hernandez DJ, Vogel KG. The in vitro interaction of proteogly-cans with type I collagen is modulated by phosphate. Arch. Biochem. Biophys. 1994; 313:102–111. [PubMed: 8053669]

Pogány G, Vogel KG. The interaction of decorin core protein fragments with type I collagen. Biochem. Biophys. Res. Commun. 1992; 189:165–172. [PubMed: 1449470]

Provenzano PP, Vanderby R. Collagen fibril morphology and organization: implications for force transmission in ligament and tendon. Matrix Biol. J. Int. Soc. Matrix Biol. 2006; 25:71–84.

Raleigh SM, van der Merwe L, Ribbans WJ, Smith RKW, Schwellnus MP, Collins M. Variants within the MMP3 gene are associated with Achilles tendinopathy: possible interaction with the COL5A1 gene. Br. J. Sports Med. 2009; 43:514–520. [PubMed: 19042922]

Riggin CN, Sarver JJ, Freedman BR, Thomas SJ, Soslowsky LJ. Analysis of collagen organization in mouse achilles tendon using high-frequency ultrasound imaging. J. Biomech. Eng. 2013

Rigozzi S, Müller R, Snedeker JG. Local strain measurement reveals a varied regional dependence of tensile tendon mechanics on glycosaminoglycan content. J. Biomech. 2009; 42:1547–1552. [PubMed: 19394024]

Robinson PS, Huang T-F, Kazam E, Iozzo RV, Birk DE, Soslowsky LJ. Influence of decorin and biglycan on mechanical properties of multiple tendons in knockout mice. J. Biomech. Eng. 2005; 127:181–185. [PubMed: 15868800]

Sarah Duenwald-Kuehl JK. Damage mechanics of porcine flexor tendon: mechanical evaluation and modeling. Ann. Biomed. Eng. 2012; 40:1692–1707. [PubMed: 22399329]

Screen HRC, Shelton JC, Chhaya VH, Kayser MV, Bader DL, Lee DA. The influence of noncollagenous matrix components on the micromechanical environment of tendon fascicles. Ann. Biomed. Eng. 2005; 33:1090–1099. [PubMed: 16133917]

September AV, Cook J, Handley CJ, van der Merwe L, Schwellnus MP, Collins M. Variants within the COL5A1 gene are associated with Achilles tendinopathy in two populations. Br. J. Sports Med. 2009; 43:357–365. [PubMed: 18443036]

Suchak AA, Bostick G, Reid D, Blitz S, Jomha N. The incidence of Achilles tendon ruptures in Edmonton, Canada. Foot Ankle Int. Am. Orthop. Foot Ankle Soc. Swiss Foot Ankle Soc. 2005; 26:932–936.

Thomopoulos S, Williams GR, Soslowsky LJ. Tendon to bone healing: differences in biomechanical, structural, and compositional properties due to a range of activity levels. J. Biomech. Eng. 2003; 125:106–113. [PubMed: 12661203]

Vogel KG, Paulsson M, Heinegård D. Specific inhibition of type I and type II collagen fibrillogenesis by the small proteoglycan of tendon. Biochem. J. 1984; 223:587–597. [PubMed: 6439184]

Xu T, Bianco P, Fisher LW, Longenecker G, Smith E, Goldstein S, Bonadio J, Boskey A, Heegaard AM, Sommer B, Satomura K, Dominguez P, Zhao C, Kulkarni AB, Robey PG, Young MF. Targeted disruption of the biglycan gene leads to an osteoporosis-like phenotype in mice. Nat. Genet. 1998; 20:78–82. [PubMed: 9731537]

Young MF, Bi Y, Ameye L, Chen X-D. Biglycan knockout mice: new models for musculoskeletal diseases. Glycoconjugate J. 2002; 19:257–262.

Zhang G, Ezura Y, Chervoneva I, Robinson PS, Beason DP, Carine ET, Soslowsky LJ, Iozzo RV, Birk DE. Decorin regulates assembly of collagen fibrils and acquisition of biomechanical properties during tendon development. J. Cell. Biochem. 2006; 98:1436–1449. [PubMed: 16518859]

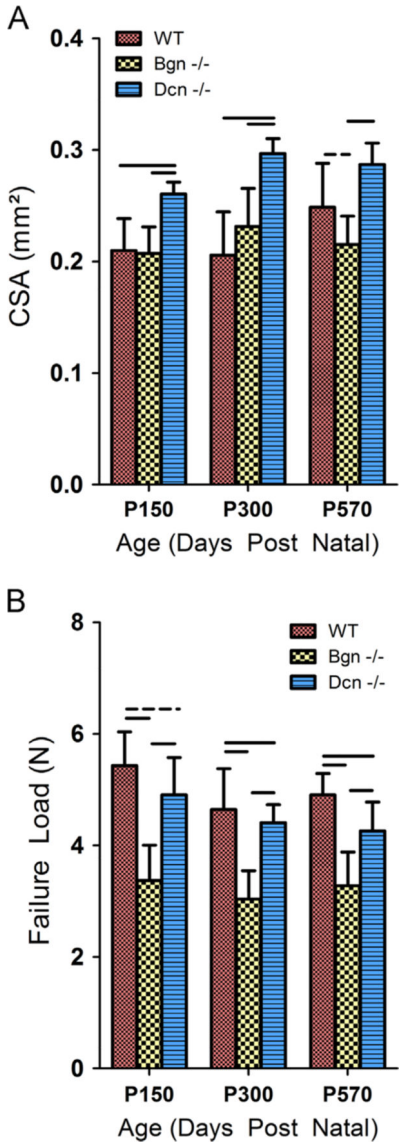

Fig. 1.

Tendon area and failure properties across genotypes and age. (A) Cross-sectional area was significantly increased in *Dcn*$^{-/-}$tendons at maturity (*P*=150) and middle age (*P*=300). This difference was not observed in old age (*P*=570). (B) In *Dcn*$^{-/-}$tendons, load at failure was significantly ($p<0.0167$) reduced in middle and old age, but only demonstrated a trend ($p<0.033$) toward reduction at maturity. *Bgn*$^{-/-}$tendons demonstrated statistically ($p<0.0167$) significant reductions at all ages. Bars indicate significant differences, dashed lines indicate trends, and error bars indicate standard deviation.

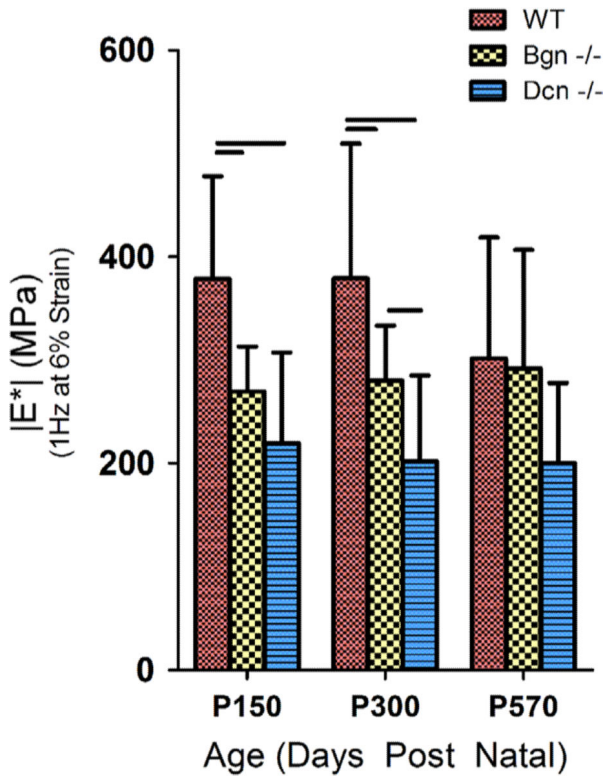

Fig. 2.

Dynamic modulus after stress relaxations tested at a frequency of 1 Hz and at 6% strain (supplemental Fig. S1 includes data from frequency sweeps including 0.1, 1, 5 and 10 Hz at 4%, 6% and 8% strain). Dynamic modulus was reduced in $Dcn^{-/-}$and $Bgn^{-/-}$mice at maturity (P=150). Reduction persisted through middle age (P=300) in both $Dcn^{-/-}$and $Bgn^{-/-}$tendons, however no significant difference was observed in any of the tendons in old age (P=570). Bars indicate significant differences (p<0.0167) and error bars indicate standard deviation.

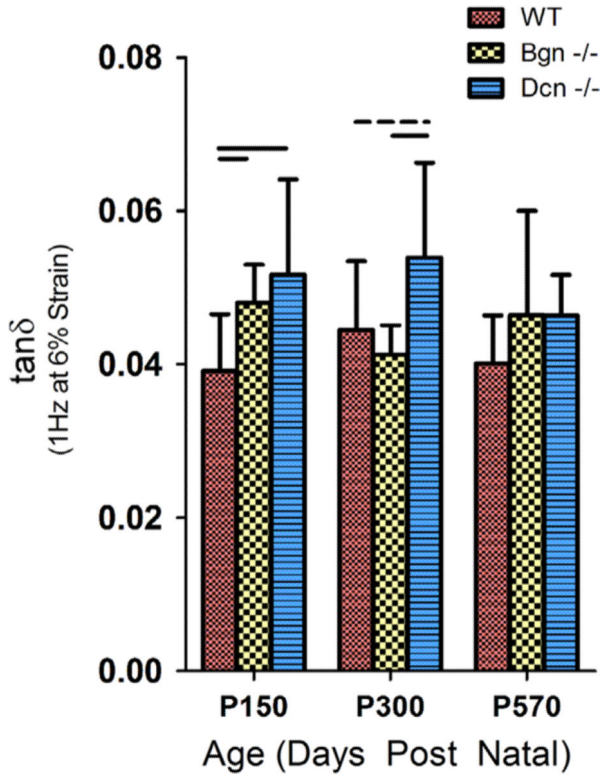

Fig. 3.

tan δ of Achilles tendon specimens after stress relaxations at 1 Hz and 6% strain (supplemental Fig. S2 includes data from frequency sweeps including 0.1, 1, 5 and 10 Hz at 4%, 6% and 8% strain) from mice at maturity, middle, and old age. We observed a general increase in tanδ for both $Dcn^{-/-}$and $Bgn^{-/-}$ tendons in a strain and frequency dependent manner. Again we observed a similar pattern in which differences found at maturity were progressively extinguished during the aging process. $Bgn^{-/-}$tendons were observed to have increased tanδ at maturity, however this difference was extinguished more rapidly than with $Dcn^{-/-}$tendons, with no significant differences observed in middle age. Bars indicate significant differences ($p<0.0167$), dashed lines indicate trends ($p<0.033$), and error bars indicate standard deviation.

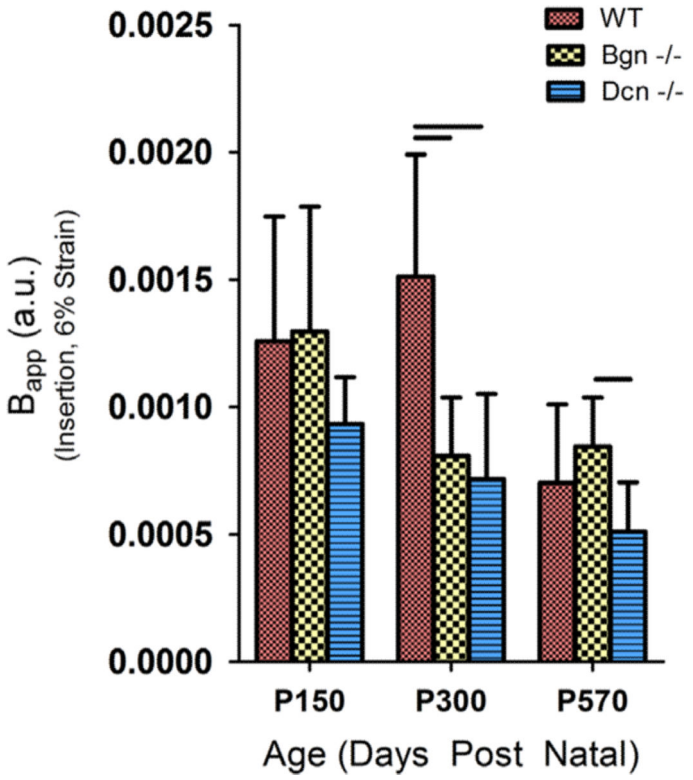

Fig. 4.

The apparent birefringence (B_{app}) measured at maturity, middle and old age during stress relaxations at 6% strain. B_{app} measured at the insertion was found to be significantly increased in WT tendons at middle age but not at maturity or in old age. This response was generally true at other strains evaluated (Fig. S3). Bars indicate significant differences ($p<0.0167$) and error bars indicate standard deviation.

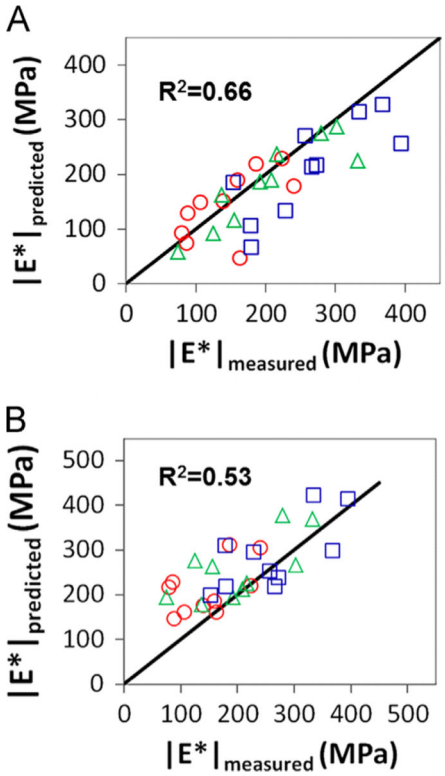

Fig. 5.

Predictions of the dynamic modulus using empirical modeling. (A) The predicted dynamic modulus, $|E^*|$, using the ratio of damaged to undamaged equilibrium stress at 6% strain for the damage coefficient, D, had a moderate coefficient of determination (R^2=0.66) to the experimentally measured $|E^*|$. (B) The predicted dynamic modulus, $|E^*|$, using the ratio of damaged to undamaged apparent birefringence, B_{app} at 6% strain for the damage coefficient, D, had a moderate coefficient of determination (R^2=0.53) to the experimentally measured $|E^*|$. Red circles represent 4% strain, green triangles represent 6% strain, and blue squares represent 8% strain. (For interpretation of the references to color in this figure legend, the reader is referred to the web version of this article.)

Table 1

Coefficients of determination and *p*-values for prediction of dynamic moduli using stress equilibrium at 6% strain as input, and reported separately for stress relaxations at 4%, 6% and 8% strain, for $Dcn^{-/-}$ tendons using model parameters derived from $Bgn^{-/-}$ tendons. We observed statistically significant correlation when comparing measured vs. predicted dynamic modulus, $|E^*|$, at 6% and 8% strain.

Parameter	Strain	R^2	*p*
$\|E^*\|$	4%	0.40	0.05
	6%	0.80	< 0.01
	8%	0.64	< 0.01
	All	0.66	< 0.01

Table 2

Coefficients of determination and *p* values for prediction of dynamic moduli using birefringence (B_{app}) as input, and reported separately for stress relaxations at 4%, 6% and 8% strain, for $Dcn^{-/-}$ tendons using model parameters derived from $Bgn^{-/-}$ tendons. We observed statistically significant correlation when comparing measured vs. predicted dynamic modulus, |*E**|, at 6% and 8% strain.

Parameter	Strain	R^2	*p*
|*E**|	4%	0.32	0.09
	6%	0.47	0.03
	8%	0.48	0.03
	All	0.53	<0.01